

Article

Preparation and Self-Repairing Properties of MF-Coated Shellac Water-Based Microcapsules

Yijuan Chang ¹ and Xiaoxing Yan ^{1,2,*}

¹ College of Furnishings and Industrial Design, Nanjing Forestry University, Nanjing 210037, China; changyijuan@njfu.edu.cn

² Co-Innovation Center of Efficient Processing and Utilization of Forest Resources, Nanjing Forestry University, Nanjing 210037, China

* Correspondence: yanxiaoxing@nuaa.edu.cn; Tel.: +86-25-85427528

Received: 8 July 2020; Accepted: 7 August 2020; Published: 10 August 2020



Abstract: A self-repairing microcapsule was prepared by emulsion polymerization using melamine formaldehyde resin (MF) as wall material, and a mixture of shellac solution and water-based coating as core material. The orthogonal experiment was carried out through five factors and four levels. The effects of $W_{\text{core}}:W_{\text{wall}}$, $W_{\text{emulsifier}}:W_{\text{core}}$, stirring rate, $W_{\text{shellac}}:W_{\text{coating}}$, $W_{\text{emulsifier solution}}:W_{\text{core}}$ on the output and coverage rate of microcapsules were studied. The stirring rate has a great influence on the preparation process of the MF-coated shellac water-based microcapsules. When the $W_{\text{core}}:W_{\text{wall}}$ is 0.8:1, $W_{\text{emulsifier}}:W_{\text{core}}$ is 3:100, stirring rate is 600 rpm, $W_{\text{shellac}}:W_{\text{coating}}$ is 1:1, $W_{\text{emulsifier solution}}:W_{\text{core}}$ is 9:1, the prepared microcapsules have the best shape and size. With the increase in concentration of microcapsules, the color difference and gloss of paint film decreased gradually. The tensile strength, scanning electron microscopy (SEM), infrared spectroscopy and repair effects of the paint film were analyzed. When the concentration of microcapsules was 5.0–10.0%, the comprehensive performance of the paint film was better, providing a technical reference for the self-repairing coatings.

Keywords: MF; shellac; water-based coating; microcapsule; self-repairing

1. Introduction

Melamine formaldehyde (MF) resin is a colorless transparent polymer obtained by reacting formaldehyde aqueous solution and melamine with distilled water under heating and stirring. Melamine can be slightly soluble in water and has good interface compatibility with water-based coating as wall material [1]. Shellac is a kind of natural and biodegradable resin [2]. It has the characteristics of low water permeability and good film formation [3], and can be solidified at room temperature. Hence, it may meet the requirements of increasingly strict environmental protection [4]. Water-based coatings have excellent mechanical properties [5], good compatibility [6], and easy modification [7]. As a one-component repair agent, water-based acrylic resin can be cured at room temperature to achieve repairs without the curing agents and additives [8], and it is suitable for the repair of water-based coatings and can improve the quality of paint films [9].

Ye et al. [10] used microcapsules to protect the encapsulation under harsh conditions and found that microcapsules have controllable loading/unloading capabilities in drug delivery and bioengineering applications. Lv et al. [11] prepared dicyclopentadiene microcapsules with phenolic resin as the wall material, and the as-prepared microcapsules can repair cement cracks. Hangari et al. [12] prepared self-healing microcapsules by coating dicyclopentadiene with nano-alumina particles modified urea-formaldehyde resin as the wall material. The results showed that the strength and heat resistance of self-healing microcapsules added with nano-alumina particles were significantly improved. Zamani et al. [13] used the in situ polymerization method to synthesize bacteria with synthetic polyurea

to repair the cement slurry. Kong et al. [14] prepared biocompatible microcapsules with shellac as wall material. The results showed that the diffusion rate of hydrophilic molecules encapsulated in the water core decreases as their molecular weight increases and the property of the microcapsules could further be modified by polyelectrolyte multilayer coating. However, these research works rarely involved the application of shellac coating, which has a significant influence on environmental protection.

When the coating cracks under stress, the microcapsules would be broken [15], then the shellac and water-based paint exude to repair cracks automatically, which can effectively prevent the propagation of microcracks, thus improving the mechanical properties of coating [16], reducing the cost of material maintenance and repair [17], and extending the service life of the coating [18,19]. The commonly used epoxy resin is cured at high temperature, but the shellac is environmentally friendly, non-toxic, cheap and can be cured at room temperature. In this paper, the MF-coated shellac water-based microcapsules were prepared by using MF as the wall material, the mixture of the shellac and water-based acrylic acid as the core material. Then, the microcapsules were added to the water-based paint to study the repair effect of the microcapsules on the paint film, to provide a practical reference for the self-repairing coatings.

2. Materials and Methods

2.1. Experimental Materials

Formaldehyde solution (37.0%, analytically pure, M_w : 30.03 g/mol, CAS No.: 50-00-0) and citric acid (M_w : 192.13 g/mol, CAS No.: 77-92-9) were supplied by XiLong Science Co., Ltd. (Shantou, China). Melamine (99.8%, M_w : 126.12 g/mol, CAS No.: 108-78-1) was provided by Shandong Ysolf Chemical Technology Co., Ltd. (Linyi, China). Triethanolamine (analytical purity, M_w : 149.19 g/mol, CAS No.: 102-71-6), ethyl acetate (M_w : 88.11 g/mol, CAS No.: 141-78-6) and anhydrous ethanol (M_w : 46.07 g/mol, CAS No.: 64-17-5) were supplied by Nanjing Chemical Reagent Co., Ltd. (Nanjing, China). The sodium dodecylbenzenesulfonate (analytical purity, M_w : 348.48 g/mol, CAS No.: 25155-30-0) and distilled water (M_w : 88.11 g/mol, CAS No.: 141-78-6) were provided by Tianjin Beichen Founder Reagent Factory (Tianjin, China). The water-based coating consists of waterborne acrylic copolymer dispersion (the concentration was 90.0%), matting agent (the concentration was 2.0%), additives (the concentration was 2.0%) and water (the concentration was 6.0%) supplied by Dulux Group (China) Co., Ltd. (Shanghai, China). Shellac (M_w : 1000 g/mol, CAS No.: 9000-59-3) was supplied by Shandong Xiangxin Chemical Co., Ltd. (Jinan, China).

2.2. Preparation of Melamine Formaldehyde (MF)-Coated Shellac Water-Based Microcapsules

An orthogonal test is based on the orthogonality to select some representative points from the comprehensive test. These representative points have the characteristics of “uniform dispersion, integrity and comparability”, which can achieve the equivalent results with a large number of comprehensive tests with the least number of tests.

The microcapsules with different particle size and morphologies were prepared by controlling the mass ratio of core wall material ($W_{\text{core}}:W_{\text{wall}}$), the mass ratio of emulsifier to core material ($W_{\text{emulsifier}}:W_{\text{core}}$), stirring rate, the mass ratio of shellac to water-based coating ($W_{\text{shellac}}:W_{\text{coating}}$), and the mass ratio of emulsifier solution to core material ($W_{\text{emulsifier solution}}:W_{\text{core}}$). W_{core} , W_{wall} , $W_{\text{emulsifier}}$, W_{shellac} , W_{coating} , and $W_{\text{emulsifier solution}}$ are the weight of the core material, wall material, emulsifier material, shellac material, coating material, and emulsifier solution material, respectively. The five-factor four-level orthogonal test (Tables 1 and 2 Nos. 11–16) was used to analyze and determine the process parameters.

- Preparation of wall material: the 15.0 g of melamine, 30.0 g of formaldehyde and 30.0 g of distilled water were weighed. After mixing, the mixture was stirred evenly, and the pH was adjusted to 8.0–9.0 by dropping triethanolamine. It was stirred and heated in a 70 °C water bath until the wall material was transparent. Then, the wall material solution was obtained by adding 45.0 g distilled water and stirred persistently for 30 min. The wall material prepolymer was obtained after natural cooling at room temperature for 10 min.
- Preparation of core material emulsion: the mixture of shellac and anhydrous ethanol according to the ratio of 1:5 was dissolved and the impurities were separated in a centrifuge. Taking the microcapsule (No. 1 in Table 2) as an example, the 4.5 g of water-based coating and 4.5 g of shellac solution were weighed and put in a beaker and stirred continuously on a blender until they were completely mixed evenly. Then, the 71.91 g of distilled water and 0.09 g of sodium dodecyl benzene sulfonate powder (as emulsifier) were mixed and stirred into emulsifier solution. The emulsifier solution was dropped into the mixture of shellac and water-based paint, stirred at 70 °C in a water bath for 60 min at 600 rpm, and the core material emulsion was obtained. Other samples refer to the preparation method of Sample 1.
- Preparation of microcapsules: the cooled melamine wall material was slowly added to the core material emulsion at a certain speed of 400, 600, 800, and 1000 rpm, respectively, and then the citric acid was added to the mixed solution to adjust the pH value to 2.5–3.0. The mixture was slowly heated to 70 °C and stirred for 3 h. The resulting product was rinsed and filtered by deionized water and anhydrous ethanol many times after being aged for 7 days at room temperature. Finally, the remaining product was put into an oven at 40 °C for heating and drying for 48 h, and the white powder obtained was the MF-coated shellac water-based microcapsules (Figure 1). The output is 25.0–38.0 g. Based on orthogonal experiment, the single factor experiment was carried out (Nos. 17–20 in Table 2), whereas the mixing speed was different.

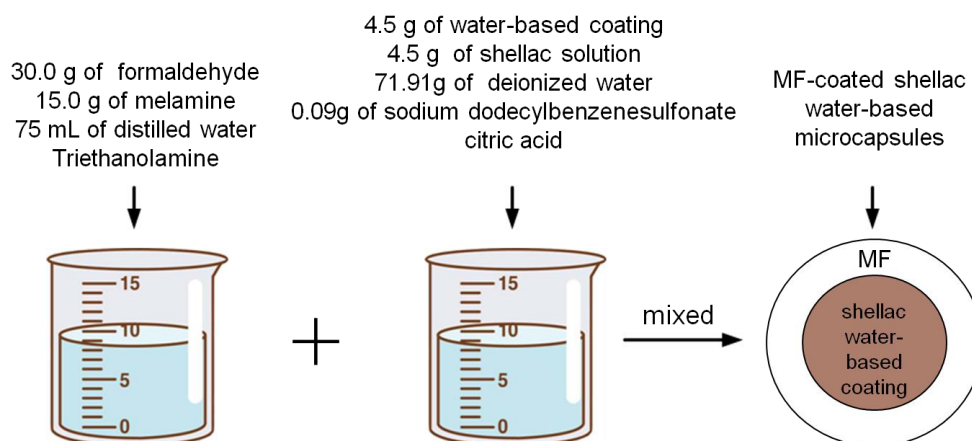


Figure 1. Schematic diagram of melamine formaldehyde (MF)-coated shellac water-based microcapsules.

Table 1. Influencing factors and levels.

Level	A $W_{\text{core}}:W_{\text{wall}}$	B $W_{\text{emulsifier}}:W_{\text{core}}$	C Stirring Rate (rpm)	D $W_{\text{shellac}}:W_{\text{coating}}$	E $W_{\text{emulsifier solution}}:W_{\text{core}}$
1	0.6:1	1:100	400	1:1.0	8:1
2	0.8:1	3:100	600	1:1.5	9:1
3	1.0:1	5:100	800	1:2.0	10:1
4	1.2:1	7:100	1000	1:2.5	11:1

Table 2. Experimental design.

Sample No.	A $W_{\text{core}}:W_{\text{wall}}$	B $W_{\text{emulsifier}}:W_{\text{core}}$	C Stirring Rate (rpm)	D $W_{\text{shellac}}:W_{\text{coating}}$	E $W_{\text{emulsifier solution}}:W_{\text{core}}$
1	0.6:1	1:100	400	1:1.0	8:1
2	0.6:1	3:100	600	1:1.5	9:1
3	0.6:1	5:100	800	1:2.0	10:1
4	0.6:1	7:100	1000	1:2.5	11:1
5	0.8:1	1:100	600	1:2.0	11:1
6	0.8:1	3:100	400	1:2.5	10:1
7	0.8:1	5:100	1000	1:1.0	9:1
8	0.8:1	7:100	800	1:1.5	8:1
9	1.0:1	1:100	800	1:2.5	9:1
10	1.0:1	3:100	1000	1:2.0	8:1
11	1.0:1	5:100	400	1:1.5	11:1
12	1.0:1	7:100	600	1:1.0	10:1
13	1.2:1	1:100	1000	1:1.5	10:1
14	1.2:1	3:100	800	1:1.0	11:1
15	1.2:1	5:100	600	1:2.5	8:1
16	1.2:1	7:100	400	1:2.0	9:1
17	0.8:1	3:100	400	1:1.0	9:1
18	0.8:1	3:100	600	1:1.0	9:1
19	0.8:1	3:100	800	1:1.0	9:1
20	0.8:1	3:100	1000	1:1.0	9:1

2.3. Preparation of Coating

The microcapsules obtained at four different stirring rates (400, 600, 800, 1000 rpm) were added to the water-based paint to form paint film with the mass fractions of 0, 5.0%, 10.0%, 15.0%, 20.0%, 25.0%, and 30.0%, respectively. The water-based paint containing microcapsules was coated on the glass substrate. The thickness of the coating was about 60 μm . The coated glass substrate was dried at room temperature for 20 min, then shifted into a 35 $^{\circ}\text{C}$ oven for heating and drying until the mass does not change, and the coating was prepared after natural cooling.

2.4. Testing and Characterization

The dried microcapsule powder was directly weighed and recorded for the output test. The 1.0 g of microcapsules was weighed, fully ground, placed in glassware. The microcapsules were fully soaked by adding ethyl acetate for 48 h and ethanol for 48 h, washed with deionized water, dried at 40 $^{\circ}\text{C}$ for 24 h and the remaining wall material can be obtained. The coverage rate was calculated according to Equation (1):

$$c = \frac{m_1 - m_2}{m_1} \times 100\% \quad (1)$$

where c is the coverage rate of microcapsules, %; m_1 is the initial mass of microcapsule, g; m_2 is the remaining wall material quality, g. The paint film was scratched with a blade, and the repair effect was observed with a ZEISS light microscope AX10 (Carl Zeiss AG, Aalen, Germany) after 7 days. The software used for morphometry is Axio Vision (Carl Zeiss AG). The SEGT-J portable color difference meter (Zhuhai Tianchuang Instrument Co., Ltd., Zhuhai, China) was used to measure the color value of the water-based paint film added with microcapsules according to GB/T 11186.3-1989 [20]. L^* represents lightness, a^* represents the change of color from red to green, b^* represents the change of color from yellow to blue, c represents the color saturation, H represents the hue. $L_1^*, a_1^*, b_1^*, c_1, H_1$ are the chromaticity values without adding the microcapsule paint film, and $L_2^*, a_2^*, b_2^*, c_2, H_2$ are the chromaticity values of the adding microcapsule paint film. ΔL^* (brightness difference) = $L_1^* - L_2^*$, Δa^* (red-green color difference) = $a_1^* - a_2^*$, Δb^* (yellow-blue color difference) = $b_1^* - b_2^*$. The color difference (ΔE) is calculated according to Equation (2).

$$\Delta E \text{ (color difference)} = [(\Delta L^*)^2 + (\Delta a^*)^2 + (\Delta b^*)^2]^{1/2} \quad (2)$$

According to GB/T 4893.6-2013 [21] Test of surface coatings of furniture-Part 6: Determination of gloss value, the gloss of paint film was measured by HG268 intelligent gloss meter (Shenzhen 3nh Technology Co., Ltd., Shenzhen, China) and the gloss of paint film is recorded at 20°, 60°, and 85° incident angles. According to ASTM D 882-02 [22], AG-IC100KN precision electronic universal testing machine (Kyoto Shimadzu Co., Ltd., Kyoto, Japan) was used to measure the tensile strength of the coating. Quanta-200 scanning electron microscope (SEM, FEI Company, Hillsboro, OR, USA) was used to analyze the morphology of microcapsule and water-based paint film. The samples adhered to the sample pedestal, and the appropriate time and voltage of gold plating were set for gold plating. After the gold plating was finished, the samples were taken out and placed in the sample chamber. When the vacuum degree reached a certain value, the pressure was increased and the SEM of the samples was observed. The acceleration voltage of SEM is 200 V–30 kV, the magnification is 20–300,000 times, and the resolution is 3.5 nm. A ZEISS light microscope AX10 (Carl Zeiss AG.) was used to analyze the surface of microcapsules and water-based paint film with microcapsules. The composition of the microcapsule and coating were tested by the VERTEX 80V infrared spectrometer (Germany Bruker Co., Ltd., Karlsruhe, Germany). The roughness of the paint films was measured by a JB-4C roughness meter (Shanghai Taiming Optical Instrument, Shanghai, China). All experiments were repeated four times with an error of less than 5.0%.

3. Results and Discussion

3.1. Morphological Analysis of Microcapsules for the Orthogonal Test

As can be seen from Figure 1, the preparation of No. 1 microcapsules was successful, but the surface is not smooth enough. The flocculation, adhesion and agglomeration were formed between microcapsules. The diameter of the microcapsule is about 6 μm . The preparation of No. 2 microcapsules was successful, but the microcapsules varied in size and had obvious adhesion. The preparation of No. 3 microcapsules was successful. Some of the microcapsules had large particles and agglomeration. The diameter of the microcapsules was about 11 μm . The size of No. 4 microcapsule was different and there was obvious agglomeration. The diameter of the microcapsules is about 12 μm . The microcapsules of No. 5 are agglomerated, and the diameter of the microcapsules is about 3 μm . The surface of No. 6 microcapsules is not smooth enough. There are a few flocs and less agglomeration, and the diameter of small microcapsules is about 3 μm . The surface of No. 7 microcapsules is smooth, a small number of small microcapsules are attached to the large microcapsules, and the diameter of the large microcapsules is about 10 μm . The microcapsules of No. 8 had agglomeration phenomenon, the size is relatively uniform, and the diameter of the microcapsule is about 13 μm . No. 9 has an agglomeration phenomenon, the size is relatively uniform, and the diameter of the microcapsule is about 5 μm . The reunion phenomenon of No. 10 is not obvious, the size of the microcapsules is relatively uniform, and the diameter is about 10 μm . The size of No. 11 microcapsule is relatively uniform, and the diameter of the microcapsule is about 5 μm . The size of No. 12 microcapsules is relatively uniform and there is adhesion. The diameter of the microcapsules is about 5–7 μm . The size of the No. 13 microcapsules is relatively uniform, with agglomeration, and the diameter of the microcapsules is about 5 μm . No. 14 microcapsules have different shapes, and some of them are not covered successfully. The diameter of the microcapsules is about 12 μm . The size of the No. 15 microcapsules is relatively uniform, with agglomeration, and the diameter of the microcapsules is about 4 μm . The size of No. 16 microcapsules is relatively uniform, and some large microcapsules are formed. The diameter of the microcapsules is about 4 μm , and the fluffy feeling is strong for No. 16. Figure 2 showed that most of the microcapsules were successfully prepared and the particle size was 3–10 μm . The morphology of the microcapsules is different due to the different core wall ratio, stirring rate and emulsifier concentration.

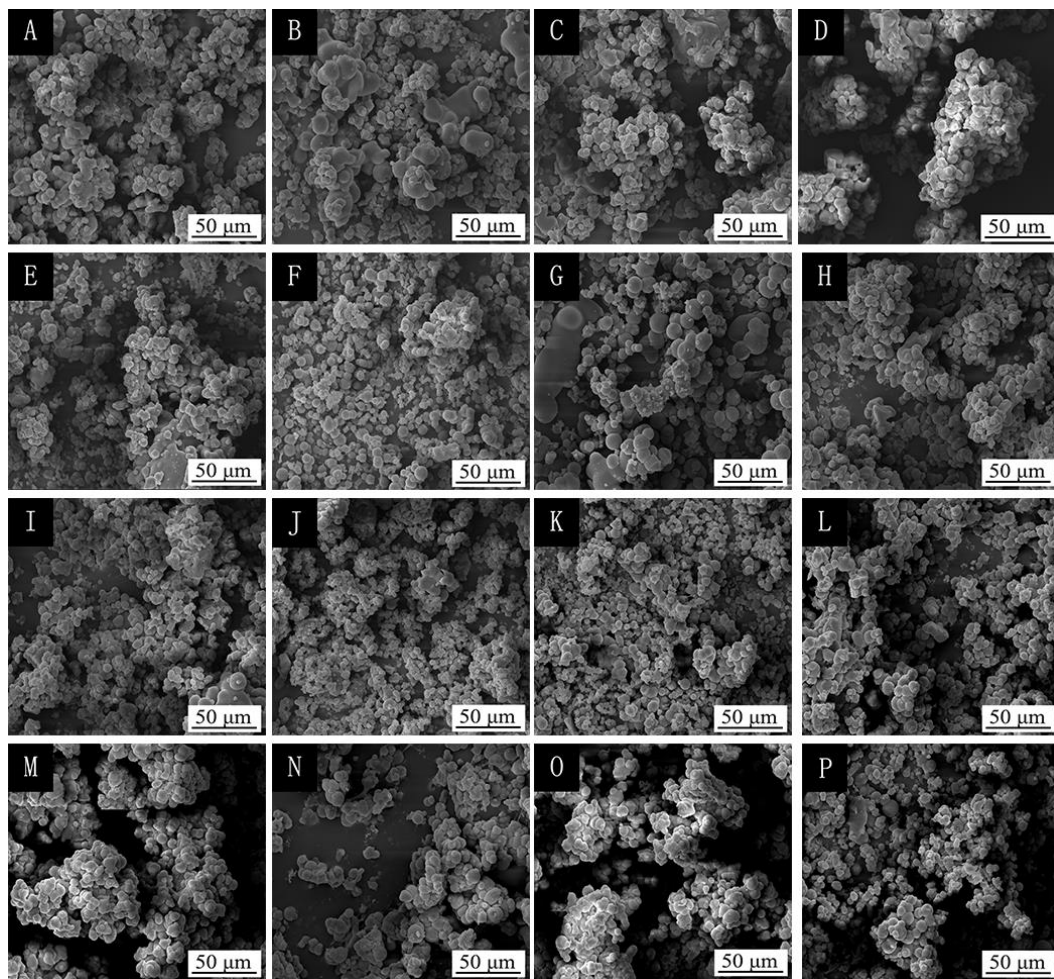


Figure 2. Scanning electron microscope (SEM) images of microcapsules obtained from the orthogonal test: (A–P) correspond to Samples 1–16 in the orthogonal test of Table 2.

The optical micrograph (OM) of microcapsules is shown in Figure 3. The microcapsules display different colors with gray and bright areas, indicating that the composition of the wall material and core material is different. The phenomenon of light diffraction ring appears in the microcapsule, which suggests that there are two different media in the microcapsule. The transparent outer ring represents the wall material, and the inner dark ring represents the core material, which is nearly circular, forming a visible core wall structure.

Table 3 shows the results of the output and coverage rate of microcapsules obtained by the orthogonal test. The output and coverage rates of the Nos. 13–16 microcapsules are high. The reason is that the quality of the core material is high, so the output is higher than Sample Nos. 1–12. Table 4 shows the range and variance results of the yield corresponding to Nos. 1–16 in Table 3. The range is represented by R , which is used to represent the difference between the maximum and minimum of the variance in statistical data. The variance in statistics (sample variance) is the average of the square of the difference between each sample value and the average of all sample values. The variance of $W_{\text{core}}:W_{\text{wall}}$ is large, so the $W_{\text{core}}:W_{\text{wall}}$ has the most significant influence on the output. The main order that affects the process conditions of the MF-coated shellac water-based coating microcapsules is $A > B > C > E > D$, and the preferred preparation process of MF-coated shellac water-based microcapsules is $A_4B_4C_1D_2E_2$.

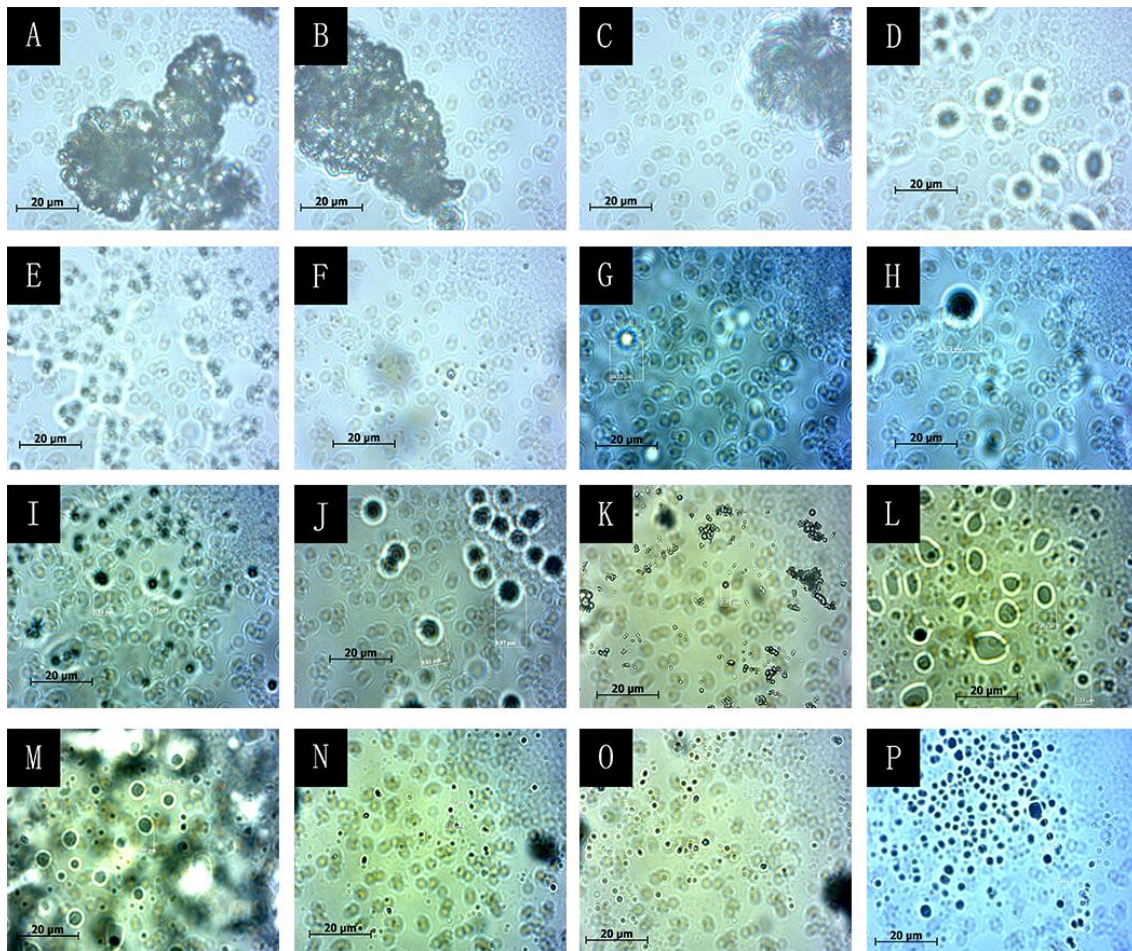


Figure 3. Optical micrograph (OM) of microcapsules: (A–P) correspond to Samples 1–16 in the orthogonal test of Table 2.

Table 3. Output and coverage rate of microcapsules.

Sample No.	Output (g)	Coverage Rate (%)
1	29.81	30.0
2	28.39	23.0
3	25.51	21.0
4	30.05	13.0
5	27.65	15.0
6	29.42	30.0
7	28.83	30.0
8	29.84	18.0
9	29.32	23.0
10	28.54	24.0
11	28.70	21.0
12	28.59	21.0
13	36.50	22.0
14	30.29	23.0
15	31.56	18.0
16	37.25	24.0
17	28.89	9.0
18	30.56	24.0
19	35.21	15.0
20	40.25	43.0

Table 4. Range and variance results of the output in the orthogonal experiment.

Horizontal	A	B	C	D	E
Mean	$W_{\text{core}}:W_{\text{wall}}$	$W_{\text{emulsifier}}:W_{\text{core}}$	Stirring Rate (rpm)	$W_{\text{shellac}}:W_{\text{coating}}$	$W_{\text{emulsifier solution}}:W_{\text{core}}$
Mean 1	28.44	30.82	31.30	29.38	29.94
Mean 2	28.94	29.16	29.05	30.86	30.95
Mean 3	28.79	28.65	28.74	29.74	30.01
Mean 4	33.90	31.43	30.98	30.09	29.17
Range	5.46	2.78	2.56	1.48	1.78
Variance	80.988	21.006	20.525	4.781	6.342

It can be seen from the results of the range and variance of the coverage rate (Table 5) that the stirring rate has the most significant effect on the microcapsules. The preferred preparation process for MF-coated shellac water-based microcapsules is $A_2B_2C_1D_1E_2$. According to the results of orthogonal experiment analysis of yield and coverage rate, the stirring rate had the most considerable influence on microcapsules.

Table 5. Range and variance of the coverage rate of microcapsules.

Horizontal	A	B	C	D	E
Mean	$W_{\text{core}}:W_{\text{wall}}$	$W_{\text{emulsifier}}:W_{\text{core}}$	Stirring Rate (rpm)	$W_{\text{shellac}}:W_{\text{coating}}$	$W_{\text{emulsifier solution}}:W_{\text{core}}$
Mean 1	21.750	22.500	26.250	26.000	22.500
Mean 2	23.250	25.000	19.250	21.000	25.000
Mean 3	22.250	22.500	21.250	21.000	23.500
Mean 4	21.750	19.000	22.500	21.000	18.000
Range	1.500	6.000	7.000	5.000	7.000
Variance	6.000	73.000	104.000	75.000	109.000

3.2. Analysis of Single Factor Test Results

According to the output and the coverage rate, the $W_{\text{core}}:W_{\text{wall}} = 0.8:1$, $W_{\text{emulsifier}}:W_{\text{core}} = 3:1$, $W_{\text{shellac}}:W_{\text{coating}} = 1:1$, $W_{\text{emulsifier solution}}:W_{\text{core}} = 9:1$ are four influencing factors, so the stirring rate is a variable, and the other four factors are fixed factors for single factor optimization test (Nos. 17–20 in Table 2). It can be seen from Table 3 (Nos. 17–20) that with the increase of the stirring rate, the output of microcapsules is increasing, but the change of the coverage rate is irregular. The sample yield and coverage rate of the No. 20 microcapsule are the highest, because of the increasing stirring speed, the mass transfer speed also increases, which makes the probability of ion collision nucleation in the solution increase.

3.3. Analysis of Micro-Morphology of Microcapsules

In Figures 4 and 5, the particle size of the microcapsules prepared at a stirring rate of 400 rpm is different, there are many small microcapsules attached to the surface of the large microcapsules, and some of them are not coated successfully. This is due to the fact that the stirring rate is too slow, resulting in insufficient power of the microcapsules [23]. In Figures 4B and 5B, microcapsules are regular spheres with smooth surfaces and good morphology. The shape of microcapsules prepared at a stirring rate of 800 rpm is irregular and partially agglomerated. The microcapsules prepared at a stirring rate of 1000 rpm are irregular in shape and have large pieces of agglomeration and adhesion, and the fluffy feeling is strong because the halving rate is too fast, breaking the combination of microcapsules. Figure 6 is the particle size distribution diagram of the microcapsules obtained at a stirring rate of 600 rpm. Most of the microcapsules are distributed between 3–10 μm , which proved that the spherical microcapsules with uniform size were successfully synthesized. When the stirring speed is low, the circulation flow of liquid is weak, only a small part of wall material and core material are stirred, and the mixing effect is not good. At the same time, the shear force produced by the magnetic rotor is small, and the mixed solution cannot be broken into uniform balls. Even if there are more emulsifiers, they cannot play a role, and the particle size is larger. With the increase of stirring rate,

the circulation flow of liquid in the agitator is strengthened, and the core material and wall material are fully mixed. At the same time, the shear force generated by the rotor also increases, which breaks the mixed solution into small and uniform balls, so the particle size is small. Therefore, 600 rpm is the most suitable stirring rate.

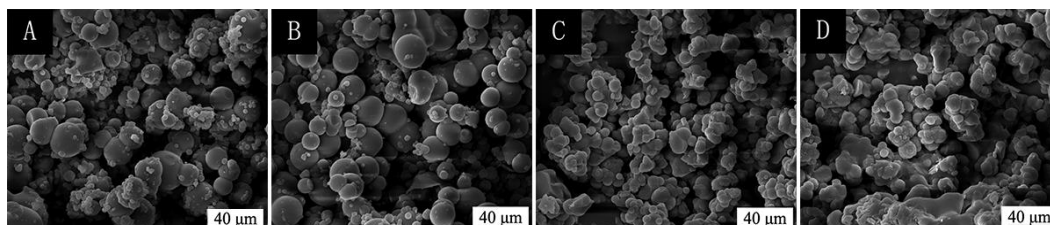


Figure 4. SEM picture of single factor test: (A) 400 rpm; (B) 600 rpm; (C) 800 rpm; (D) 1000 rpm.

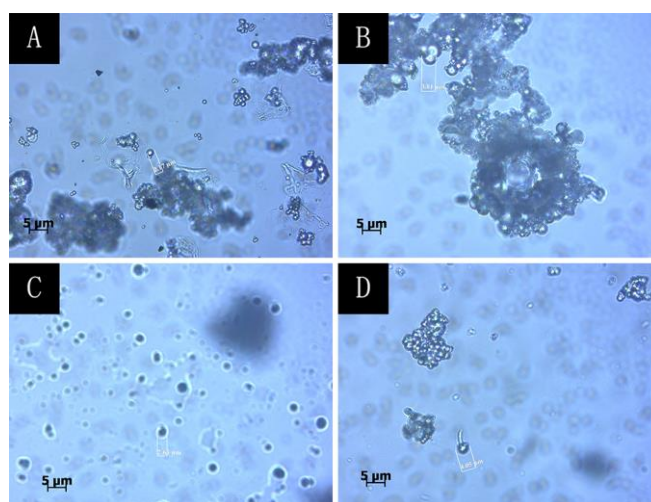


Figure 5. OM of single factor test: (A) 400 rpm; (B) 600 rpm; (C) 800 rpm; (D) 1000 rpm.

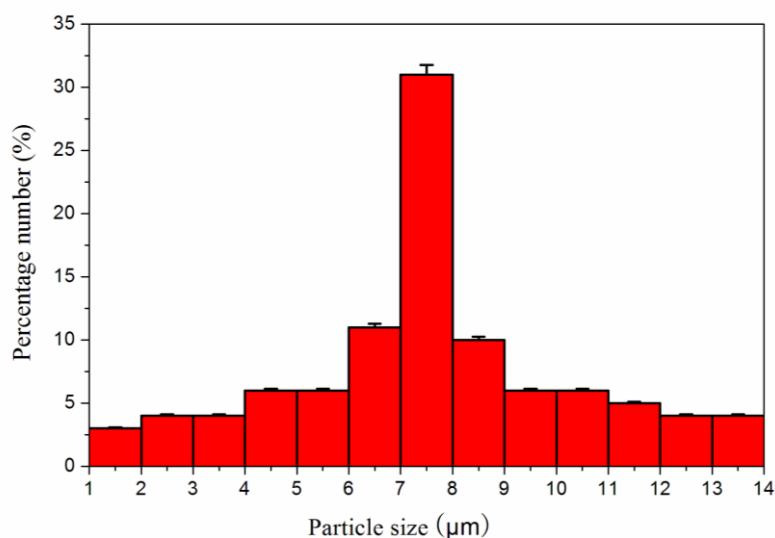


Figure 6. The particle size distribution of microcapsules (Sample 18 in Table 3).

3.4. Analysis of the Chemical Composition of Microcapsules

Figure 7 is the infrared spectrum of four microcapsules prepared by the independent optimization test. Peaks at 3400, 2930, 1570 and 1344 cm^{-1} are the stretching vibration absorption peaks of the N–H,

C–H, C=N, and C–N bonds. The 2930, 3383 cm^{-1} are the $-\text{CH}_2$, $-\text{OH}$ in microcapsules and shellac. The absorption at 1726 cm^{-1} represents the characteristic peak of C=O in the water-based acrylic resin. The absorption at 1750 cm^{-1} is the COOH group in shellac. The absorption of COOH functional group in shellac and C=O bond in the water-based acrylic resin appeared at 1750 cm^{-1} and 1726 cm^{-1} for the four kinds of microcapsules (Samples 17–20 in Table 2), indicating that the shellac and water-based acrylic resin were successfully coated. The infrared absorption trend of the four microcapsules is consistent, indicating that there is no difference in the composition of the four microcapsules with different stirring rates.

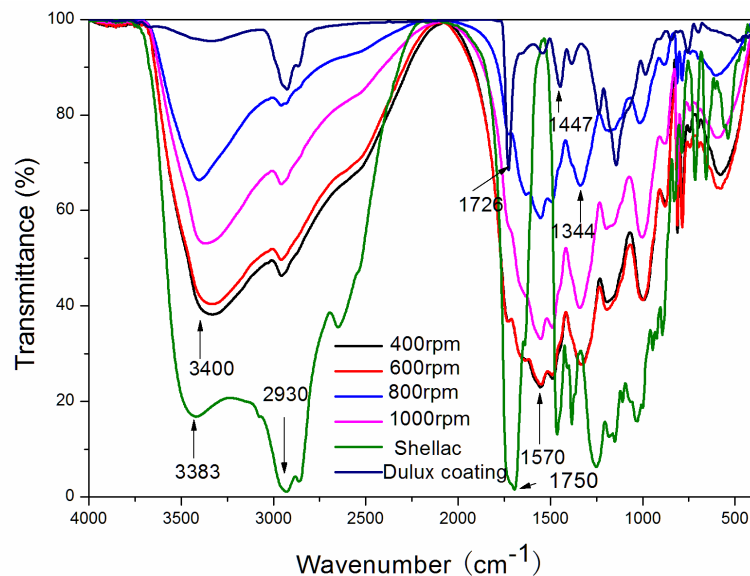


Figure 7. Single factor infrared spectroscopy.

3.5. Effect of Microcapsule Mass Fraction on Color Difference

The effect of the concentration of microcapsules with different stirring rates on the color difference of the paint film is shown in Figure 8. With increasing the concentration of microcapsules from 400–800 rpm, the color difference of the paint film gradually increases, mainly because the increase of microcapsule particles and the uneven surface of the paint film. The microcapsules prepared by 1000 rpm have a strong fluffy feeling and can be easily solidified into blocks when added into the water-based paint film. As a result, the surface of the paint film is uneven and the color difference changes irregularly. The color difference of the microcapsule paint film added with different stirring rates is not much different. The reason is that the MF-coated shellac water-based microcapsules are a white split. As the mass fraction of microcapsules increases, the brightness of the paint film increases, but the values of red green and yellow blue did not change much, so the color difference with different mass fractions of microcapsules is not very different.

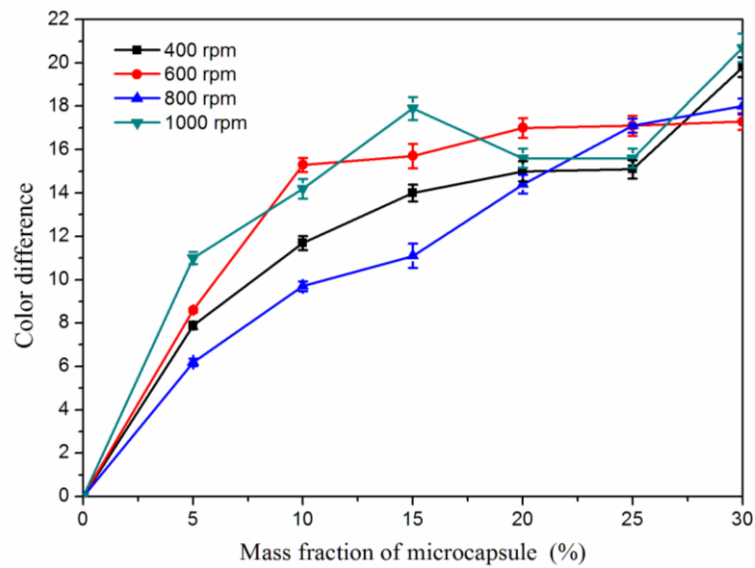


Figure 8. Influence of microcapsule mass fraction at different stirring rates on the color difference of paint film.

3.6. Effects of Microcapsule Mass Fractions on the Gloss and Roughness

The gloss of the coating with microcapsules obtained at different stirring rates was measured at three incident angles of 20° , 60° , and 85° . As can be seen from Figure 9, as the mass fraction of microcapsules increases, the gloss gradually decreases. This is because the increase in the mass fraction of microcapsules increases the roughness (Figure 10) of the surface of the paint film [24], and the rise in surface particles leads to the enhancement of the diffuse reflection phenomenon on the coating surface [25], thereby reducing the gloss of the paint film. The more microcapsules are added, the more uneven the film surface and the greater the roughness.

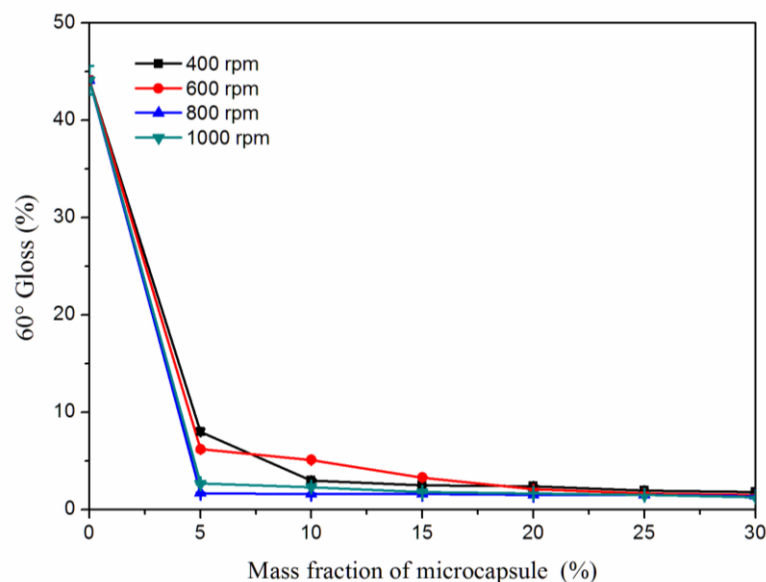


Figure 9. Effect of the mass fractions of microcapsules with different stirring rates on the gloss of water-based paint film.

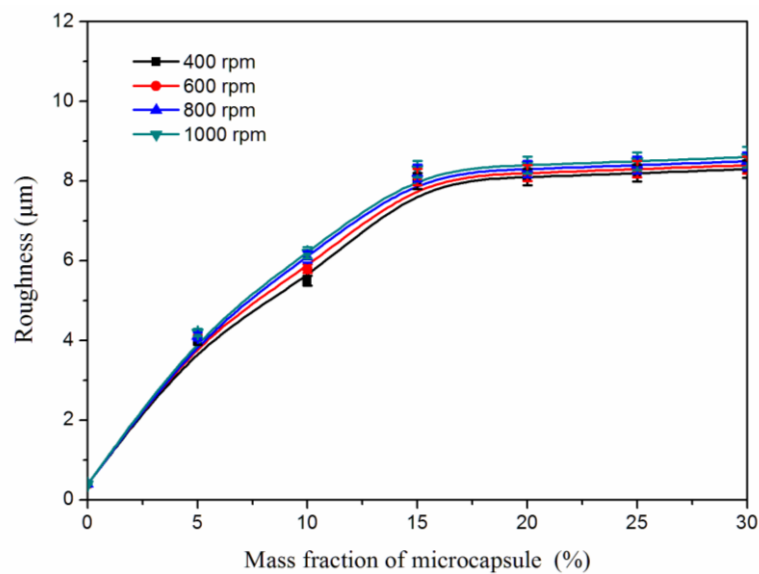


Figure 10. Effect of the mass fractions of microcapsules with different stirring rates on the roughness of water-based paint film.

3.7. Effect of Microcapsule Mass Fractions at Different Stirring Rates on Tensile Strength

Figure 11 is the SEM picture of the coating with the different mass fractions of microcapsules obtained at 600 rpm. It can be seen from Figure 11 that the paint film without microcapsules is flat and smooth. The paint film with 5.0–10.0% microcapsule mass fraction has a small number of particles, and the surface of the paint film is relatively uniform. The paint film with a microcapsule mass fraction of 30.0% has a large particle distribution, and the paint film is cracked. When the mass fraction of microcapsules is 0–10.0%, the surface of paint film is relatively flat. If microcapsules are added too much, it will not only affect the surface quality of the paint film, but also reduce the aesthetics.

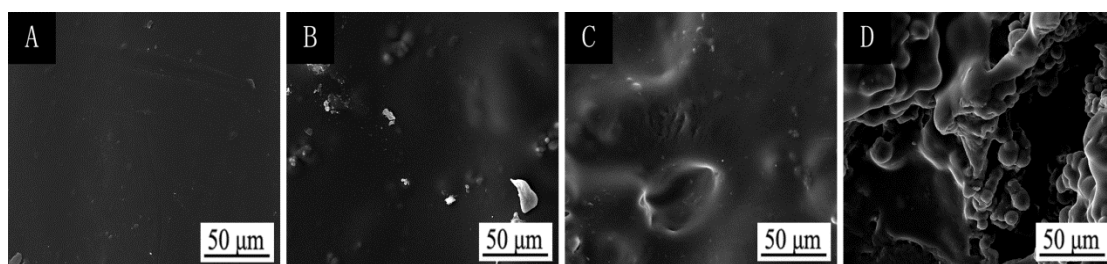


Figure 11. SEM image of water-based paint film with different mass fractions: (A) 0; (B) 5.0%; (C) 10.0%; (D) 30.0%.

It can be seen from Figure 12 that the tensile strength of the microcapsules prepared at 400, 800, and 1000 rpm were not substantially enhanced. With the addition of 600 rpm, the tensile strength of the paint film increased first and then decreased. The reason is that the more microcapsules added in the coating, the more uneven the dispersion is and the greater the agglomeration is. When the stirring rate is 600 rpm and the mass fraction of the microcapsule is 5.0%, the maximum tensile strength of the paint film is 21.22 N/mm. When the mass fraction is 10.0%, the maximum tensile strength is 20.91 N/mm. At this time, the microcapsule particles are dispersed more evenly (Figure 11) and the tensile strength is better. When the mass fraction of microcapsules is appropriate, the film will play a certain role in pinning, so the tensile strength of the film increases. When the microcapsules are added too much and the water-based coatings are too few, the solid particles on the surface of the paint film increase and the gap between the particles will also increase, so the tensile strength of the film will be reduced.

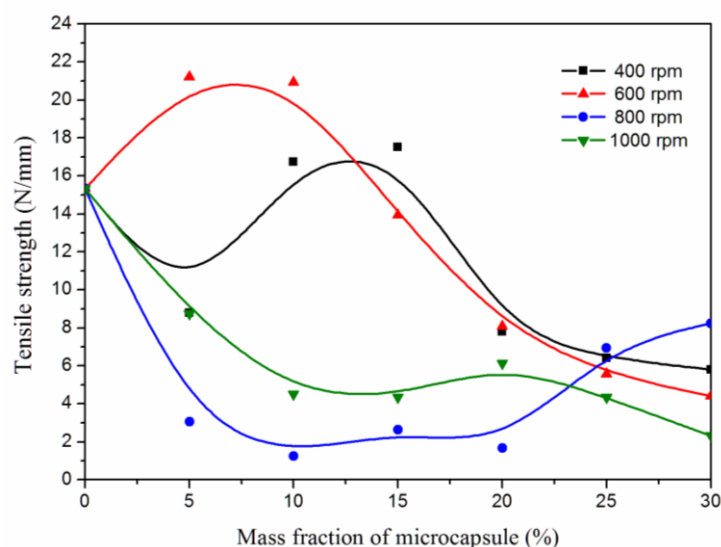


Figure 12. Effect of the mass fraction of microcapsules with different stirring rates on the tensile strength of water-based paint film.

Figure 13 shows the infrared spectrum of microcapsules prepared at a stirring rate of 600 rpm, and the water-based paint with different mass fractions of the microcapsules. The characteristic absorption peak of C–H appears around 1447 cm^{-1} . The 2930 , 1600 and 1542 cm^{-1} stretching vibration absorption peaks are the $-\text{CH}_2$, $\text{C}=\text{N}$, and $\text{N}-\text{H}$ bonds in melamine, respectively. The 1726 cm^{-1} represents the characteristic peak of $\text{C}=\text{O}$ in the water-based acrylic resin of the microcapsules. The 2930 , 3383 cm^{-1} are the $-\text{CH}_2$, $-\text{OH}$ in microcapsules and shellac. The infrared spectrum of coating with different mass fractions of microcapsules (5.0–30.0%) was consistent, and no peak disappeared or appeared, indicating that there was no chemical reaction between the microcapsules and the paint film. Although the components of microcapsules obtained by different stirring rates are the same, but the mass fractions of the microcapsules are different.

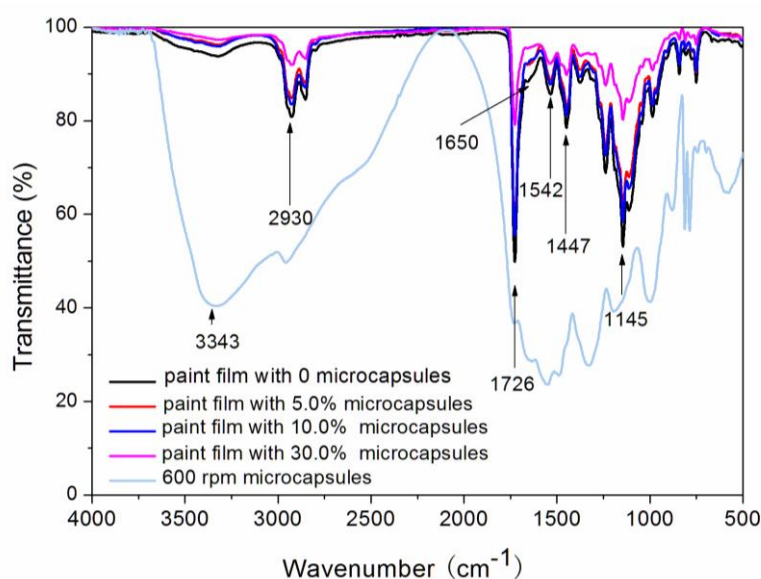


Figure 13. The infrared spectrum of water-based paint film with different microcapsule mass fractions.

3.8. Repair Ability Effect

The paint film with 5.0% and 10.0% microcapsules were cross scratched by a blade. After 7 days, the self-repairing effect of the film was observed by the microscope. It can be seen from Figure 14 that the scratch width of the paint film with a microcapsule concentration of 5.0% was repaired from the original 1.14 to 0.31 μm , while that of 10.0% was repaired from the 2.48 to 0.94 μm . It can be seen that the paint film added with microcapsules has an obvious repairing effect [26].

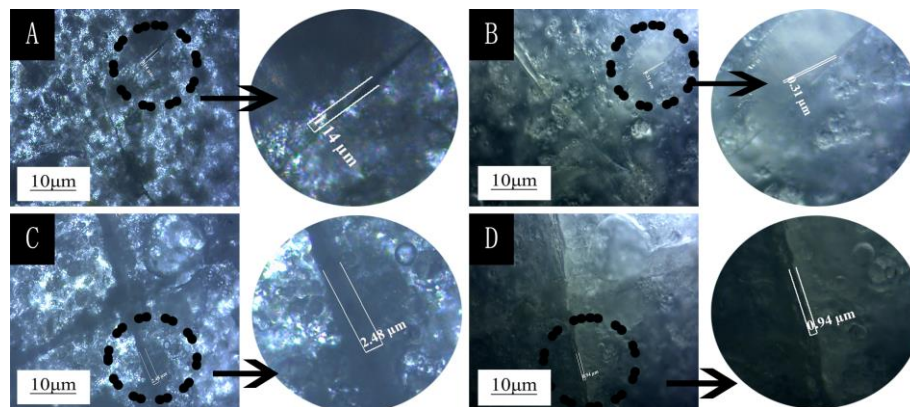


Figure 14. Effect of different microcapsule mass fractions on the repair effect of the paint film: (A,B) are the paint film before and after repairing with the microcapsule mass fraction of 5.0%; (C,D) are the paint film before and after repairing with microcapsule mass fraction of 10.0%.

4. Conclusions

The MF-coated shellac water-based microcapsules were prepared by orthogonal experiments. The comprehensive analysis of the output, coverage, range, variance, and SEM analysis showed that the biggest factor affecting the particle size of the microcapsules was the stirring rate. The best preparation parameters are: $W_{\text{core}}:W_{\text{wall}} = 0.8:1$, $W_{\text{emulsifier}}:W_{\text{core}} = 3:100$, $W_{\text{shellac}}:W_{\text{coating}} = 1:1$, $W_{\text{emulsifier solution}}:W_{\text{core}} = 9:1$, stirring rate = 600 rpm. The color difference of paint film added with the microcapsules of different stirring rates decreased with the increase of the microcapsule mass fraction, and the gloss of the paint film decreased with the rise of the microcapsule mass fraction. When the stirring speed was 600 rpm, the prepared microcapsules have good repairing effect on the paint film. For the comprehensive consideration, when the mass fraction of microcapsules is 5.0–10.0%, the paint films have a high gloss, small color difference, high tensile strength and good repairing effect. This study will lay a practical foundation for the self-repairing paint film.

Author Contributions: Conceptualization, Y.C.; methodology, Y.C.; resources, Y.C.; data curation, Y.C.; writing—original draft preparation, Y.C.; analyzed the data, Y.C.; validation investigation, X.Y.; writing—review and editing, X.Y.; supervision X.Y. All authors have read and agreed to the published version of the manuscript.

Funding: This research was funded by [Graduate Research Innovation Program of Jiangsu Province] grant number [KYCX20_0888] and [General Program of Jiangsu Natural Science Foundation in 2020] (Project title: Study on the relationship between microstructure control of self-repairing coating and wood based on microcapsule technology).

Conflicts of Interest: The authors declare no conflict of interest.

References

1. Liu, M.; Zhang, C.; Du, Z.; Zou, W. Fabrication of shape-stabilized phase change materials with melamine foam/multi-walled carbon nanotubes composite as container. *Compos. Interfaces* **2020**, 1–17. [[CrossRef](#)]
2. Morales, E.; Rubilar, M.; Burgos-Díaz, C.; Acevedo, F.; Penning, M.; Shene, C. Alginate/shellac beads developed by external gelation as a highly efficient model system for oil encapsulation with intestinal delivery. *Food Hydrocoll.* **2017**, *70*, 321–328. [[CrossRef](#)]

3. Silva, M.; Tulini, F.; Ribas, M.M.; Penning, M.; Favaro-Trindade, C.S.; Poncelet, D. Microcapsules loaded with the probiotic lactobacillus paracasei BGP-1 produced by co-extrusion technology using alginate/shellac as wall material: Characterization and evaluation of drying processes. *Food Res. Int.* **2016**, *89*, 582–590. [[CrossRef](#)] [[PubMed](#)]
4. Qi, Y.; Shen, L.; Zhang, J.; Yao, J.; Lu, R.; Miyakoshi, T. Species and release characteristics of VOCs in furniture coating process. *Environ. Pollut.* **2019**, *245*, 810–819. [[CrossRef](#)]
5. Dai, J.; Ma, S.; Liu, X.; Han, L.; Wu, Y.; Dai, X.; Zhu, J. Synthesis of bio-based unsaturated polyester resins and their application in waterborne UV-curable coatings. *Prog. Org. Coat.* **2015**, *78*, 49–54. [[CrossRef](#)]
6. Herrera, R.; Muszyńska, M.; Krystofiak, T.; Labidi, J. Comparative evaluation of different thermally modified wood samples finishing with UV-curable and waterborne coatings. *Appl. Surf. Sci.* **2015**, *357*, 1444–1453. [[CrossRef](#)]
7. Zhang, S.W.; Yu, A.X.; Song, X.Q.; Liu, X.Y. Synthesis and characterization of waterborne UV curable polyurethane nanocomposites based on the macromonomer surface modification of colloidal silica. *Prog. Org. Coat.* **2013**, *76*, 1032–1039. [[CrossRef](#)]
8. Pepin, S.; Blanchet, P.; Landry, V. Interactions between a buffered amine oxide impregnation carrier and an acrylic resin, and their relationship with moisture. *Coatings* **2020**, *10*, 366. [[CrossRef](#)]
9. Xiong, X.Q.; Yuan, Y.Y.; Niu, Y.T.; Zhang, L.T. Development of a cornstarch adhesive for laminated veneer lumber bonding for use in engineered wood flooring. *Int. J. Adhes. Adhes.* **2020**, *98*, 102534.
10. Ye, C.; Combs, Z.A.; Calabrese, R.; Dai, H.; Kaplan, D.L.; Tsukruk, V.V. Robust microcapsules with controlled permeability from silk fibroin reinforced with graphene oxide. *Small* **2014**, *10*, 5087–5097. [[CrossRef](#)]
11. Lv, L.; Yang, Z.; Chen, G.; Zhu, G.; Han, N.; Schlangen, E.; Xing, F. Synthesis and characterization of a new polymeric microcapsule and feasibility investigation in self-healing cementitious materials. *Constr. Build. Mater.* **2016**, *105*, 487–495. [[CrossRef](#)]
12. Ahangari, M.G.; Fereidoon, A.; Jahanshahi, M.; Sharifi, N. Effect of nanoparticles on the micromechanical and surface properties of poly(urea–formaldehyde) composite microcapsules. *Compos. Part. B Eng.* **2014**, *56*, 450–455. [[CrossRef](#)]
13. Zamani, M.; Nikafshar, S.; Mousa, A.; Behnia, A. Bacteria encapsulation using synthesized polyurea for self-healing of cement paste. *Constr. Build. Mater.* **2020**, *249*, 118556. [[CrossRef](#)]
14. Kong, L.; Amstad, E.; Hai, M.; Ke, X.; Chen, D.; Zhao, C.X.; Weitz, D.A. Biocompatible microcapsules with a water core templated from single emulsions. *Chin. Chem. Lett.* **2017**, *28*, 1897–1900. [[CrossRef](#)]
15. Yan, X.; Chang, Y. Investigation of waterborne thermochromic topcoat film with color-changing microcapsules on Chinese fir surface. *Prog. Org. Coat.* **2019**, *136*, 105262. [[CrossRef](#)]
16. Wu, Y.; Zhang, H.Q.; Zhang, Y.; Wang, S.Q.; Wang, X.Z.; Xu, D.L.; Liu, X. Effects of thermal treatment on the mechanical properties of larch (*larix gmelinii*) and red oak (*quercus rubra*) wood cell walls via nanoindentation. *Bioresources* **2019**, *14*, 8048–8057.
17. Xiong, X.Q.; Niu, Y.T.; Ma, Q.R.; Pan, Y.T. Study on the warm-cool and dry-wet feeling of straw board surface. *Wood Res.* **2020**, *65*, 221–230. [[CrossRef](#)]
18. Xu, W.; Fang, X.Y.; Han, J.T.; Wu, Z.H.; Zhang, J.L. Effect of coating thickness on sound absorption property of four wood species commonly used for piano soundboards. *Wood Fiber Sci.* **2020**, *52*, 28–43. [[CrossRef](#)]
19. Xiong, X.Q.; Niu, Y.T.; Yuan, Y.Y.; Zhang, L.T. Study on dimensional stability of veneer rice straw particleboard. *Coatings* **2020**, *10*, 558. [[CrossRef](#)]
20. GB/T 11186.3-1989. *Method of Measurement of Coating Color. Part III: Calculation of Chromatic Aberration*; Standardization Administration of the People's Republic of China: Beijing, China, 1990.
21. GB/T 4893.6-2013. *Test of Surface Coatings of Furniture Part 6: Determination of Gloss Value*; Standardization Administration of the People's Republic of China: Beijing, China, 2013; pp. 1–6. (In Chinese)
22. ASTM D 882-02 Standard. *Test Method for Tensile Properties of Thin Plastic Sheeting*; ASTM International: West Conshohocken, PA, USA, 2002.
23. Kong, Q.M.; Wang, X.J.; Lou, T. Preparation of millimeter-sized chitosan/carboxymethyl cellulose hollow capsule and its dye adsorption properties. *Carbohydr. Polymer.* **2020**, *244*, 116481. [[CrossRef](#)]
24. Xiong, X.Q.; Yuan, Y.Y.; Niu, Y.T.; Zhang, L.T. Research on the effects of roughness on the tactile properties of rice straw particleboard surface. *Sci. Adv. Mater.* **2020**, *12*, 795–801. [[CrossRef](#)]

25. Ueda, K.; Kanai, H.; Suzuki, T.; Amari, T. Effects of mechanical properties of paint film on the forming of pre-painted steel sheets. *Prog. Org. Coat.* **2001**, *43*, 233–242. [[CrossRef](#)]
26. Jadhav, R.S.; Hundiwale, D.G.; Mahulikar, P.P. Synthesis and characterization of phenol-formaldehyde microcapsules containing linseed oil and its use in epoxy for self-healing and anticorrosive coating. *J. Appl. Polym. Sci.* **2010**, *119*, 2911–2916. [[CrossRef](#)]



© 2020 by the authors. Licensee MDPI, Basel, Switzerland. This article is an open access article distributed under the terms and conditions of the Creative Commons Attribution (CC BY) license (<http://creativecommons.org/licenses/by/4.0/>).